

Received October 2, 2021, accepted October 30, 2021, date of publication November 8, 2021, date of current version November 22, 2021.

Digital Object Identifier 10.1109/ACCESS.2021.3126393

# Diffuse Reflectance Illumination Module Improvements in Near-Infrared Spectrometer for Heterogeneous Sample Analysis

UMACHANDI MANTENA<sup>1,2</sup>, SOURABH ROY<sup>1</sup>, AND RAMESH DATLA<sup>2</sup>

<sup>1</sup>Department of Physics, National Institute of Technology, Warangal 506004, India

<sup>2</sup>ELICO Ltd., Sanathnagar, Hyderabad 500018, India

Corresponding author: Umachandi Mantena (mumachandi@gmail.com)

**ABSTRACT** This paper presents a portable and affordable prototype using a Digital Micro-mirror Device (DMD) based Near-Infrared Spectrometer and an improved diffuse reflectance illumination module (DRIM). The improved DRIM produced optical geometry parameters such as 3.5mm standoff distance (SD), 2mm depth of overlap illumination area (DOIR), and 4mm sample active illumination area (SAIA). It enables the single and multi-point scans to determine the crude content of various food quality parameters and homogeneity by averaging spatial inhomogeneities of raw material and heterogeneous sample mixtures placed at a standoff distance. The prototype outperformed the current portable NIRS by a factor of 2-3 in terms of optical throughput, signal-to-noise ratio, and baseline. The prototype's repeatability was determined by assessing pure samples such as chalk powder, red chili powder, wheat, and groundnuts using scattering correction techniques and was computed <1% relative standard deviation (RSD). Partial least square regression (PLSR) was used to build a prediction model using around 100 randomly selected poultry feed samples with 10-20% moisture ranges-. Results of the experiments indicated values for the coefficient of determination as high as 0.991, and root mean square error was 0.32%, and a prediction accuracy with maximum deviation of <1%. The results indicated that the prototype was able to efficiently predict heterogeneous mixtures and food grains, provide new specifications for single and multi-point scan measurements, and this carries a lot of potential as a stand-alone or in-line food monitoring tool.

**INDEX TERMS** Chemometrics, diffuse reflectance, digital micromirror device, food industries, heterogeneous sample, moisture measurement, near-infrared spectrometer, partial least squares regression, predictive models, scattering correction techniques, signal-to-noise ratio.

## I. INTRODUCTION

In today's food industry, there is a requirement for a rapid, reliable, accurate, compact, and cost-effective mechanism for analysing food products using modern technology. The near-infrared spectrometer (NIRS) is a versatile analytical tool that combines chemometric techniques with the benefits of being simple, rapid, non-invasive, and non-destructive [1]–[3]. The non-destructive feature of NIRS enables food sample analysis without any prior processing [4]–[6]. To extract spectral information from the test sample, NIRS uses standard measurement modes that allow non-invasive radiation interaction with the sample. The measurement

modes are determined by the sample form or position, and the sensing wavelength region. The most common traditional measurement modes are transmittance, transreflectance, and diffuse-reflectance [7], [8]. Numerous studies have been conducted on new techniques, instrumentations, and methods to increase the ability of near-infrared (NIR) analysis to measure quality and safety parameters in a wide range of food products and processes [8]–[11]. For high-performing NIRS, improving illumination module geometries is a critical parameter [12], [13]. Experimental studies on new techniques ultimately help turn laboratory equipment into portable commercial sample estimation equipment for static and in-line analysis. As a result of these research studies, large and small-scale industries, retailers, and academia may use the latest technology.

The associate editor coordinating the review of this manuscript and approving it for publication was Md Selim Habib<sup>1</sup>.

Most NIRS instruments with a traditional grating spectrometer have a fixed grating with a linear array detector (InGaAs) or a scanning grating with a single-element detector (InGaAs). Conventional linear image sensor spectrometers are costly, have low resolution, and often need a single or multiple-stage thermoelectric cooler (TEC). Simultaneously, the mechanical structure of a scanning grating-based spectrometer with a single element detector is complex, mainly where portability is concerned [14]. Whereas a multi-point NIRS, which uses fiber probes to provide spectral and spatial information in real-time has a lot of potential in the food industry [15], [16]. A multi-point scan analysis, rather than a single-point analysis, is needed to overcome significant interference caused by water and physical attributes such as sample size, shape, and hardness [17]. A multi-point NIRS device based on a Fabry–Perot interferometer could be used in-line on dairy products for simultaneous monitoring and quality evaluation [18]. In the pharmaceutical industry, inhomogeneities in the process chamber of the hot melt coating process can be detected by placing fibers at different positions that enable multi-point NIRS measurements [19], [20]. The methods listed above can accommodate multiple fiber probes and NIR spectrometers in real-time multi-point analysis, but they are complex and expensive to use. A new digital micro-mirror device (DMD)-based NIRscan Nano Evaluation module (EVM) proposed by Texas Instruments (TI) is a viable alternative to grating-based NIRS and FT-NIRS [21] because of its high signal-to-noise ratio (SNR), wavelength selection ability, speed, mechanical stability, and low cost. The NIRscan Nano EVM is another popular and potentially useful NIRS analytical tool that can be used in single-point scan analysis in real-time when in direct contact with the test sample, but it is not suitable for single and multi-point scan analysis for a standoff distant sample. It also has other design limitations, such as depth of overlap illumination region (DOIR) and sample active illumination area (SAIA). If the discussed problems can be addressed, the performance of NIRS can significantly improve.

In this proposed work, we have overcome the challenges of TI's NIRscan Nano EVM. The first challenge is the difficulty in collecting high-quality spectral data from samples at a standoff distance. Because of the limitations of this instrument's illumination module, collecting high-quality spectral data from samples at a standoff distance is difficult. That is, it facilitates single-point analysis and allows for accurate measurements for a sample within 0.75 mm against a sapphire window but is inadequate to accommodate sample holder and sample rotation mechanisms for multi-point scan and standoff distant sample studies when the sample is placed at a distance of more than 0.75 mm from the sapphire window [22]. We propose modifying the illumination module's optical geometry to the desired standoff distance in ELICO prototype to address this problem. To optimize the illumination module and its instrumental functionality, we have

conducted research studies on SAIA, DOIR, and collection of diffuse reflected light from target samples positioned at standoff distances. The result of our studies is an improved portable ELICO NIRS prototype which allows for single and multi-point scans to average out spatial inhomogeneities of the samples like bulk and heterogeneous samples [23]. We evaluated the efficiency and efficacy of ELICO NIRS prototype to measure moisture content in feed formulation using experimental analysis and by making comparisons with existing TI's instrument NIRscan Nano EVM and the ELICO NIRS prototype.

## II. LIMITATIONS AND SCOPE OF IMPROVEMENTS

The NIR instrument design was influenced by the target sample, measurement mode, wavelength region selection, techniques, and application field [24]. To maximize the instrument's effectiveness, an NIR range of 900-1700 nm was selected. For sample content evaluation, pre-mathematical and chemometrics were used to resolve the NIR region's disadvantages, such as low structural selectivity and sample composition determination from weaker absorption overtones.

The NIRscan Nano EVM is an analytical tool that primarily consists of:

- Illumination module - used to illuminate the sample and capture diffuse reflection light.
- A polychromator with a fixed grating and a DMD that allows for wavelength selection.
- Collimated and focus optics – to guide diffused light collection.
- A single InGaAs Photodetector is used to detect light photons and convert them into electrical signals.

For the sample analysis, a diffuse reflectance illumination module in NIRscan Nano EVM was used. In this configuration, the sample was kept directly against the sapphire window. A light beam from two lens end lamps was focused on the sample, scattered within the sample, and returned to the surface after being absorbed by the sample, which is referred to as diffuse reflectance. Optics captures the diffuse reflectance and directs it toward the detector. The geometry of this configuration reduces specular reflection, which contains no chemical information. The light source and detector are placed on the same side of the sample, illuminating it at a 40-degree angle to avoid specular reflection collection. The light beam from two lens-end tungsten lamps is focused about 3mm away from the lamps, intersects at about 0.75 mm past the sapphire window, and creates a 2.5 mm diameter illumination spot where the sample is placed. The collection optics [25] capture diffused reflectance light from a 2.5 mm diameter illumination spot at the sample window. Fig. 1 shows the NIRscan Nano EVM's illumination module.

The existing illumination module has the following drawbacks:

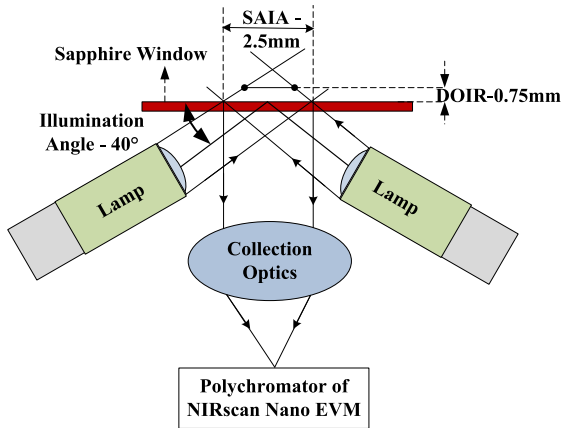


FIGURE 1. Schematic of the illumination module of the NIRscan nano EVM.

- If the sample is moved farther away from the window, the sample cannot obtain enough illumination for the device to conduct an effective scan.
- Laboratory analysis of grains and powder samples necessitates a sample holder with a thickness of around 1.5mm, producing inaccurate results.
- It enables single-point analysis of a small portion of the sample, which is difficult to do when analyzing a large number of inhomogeneous or heterogeneous products.

The above points indicate a scope to develop a new illumination module for analyzing a standoff distant sample and attempting multi-point scan analysis by scanning different sample areas consecutively to average spatial inhomogeneities.

### III. MATERIALS AND METHODS

#### A. INSTRUMENT DESIGN

Current investigations have identified limitations in existing equipment to fulfill Food industry requirements for multi-point scan analysis of standoff distant samples. Therefore, we developed a new illumination module and integrated it with the NIRscan Nano EVM’s polychromator for this prototype. This illumination module was made with two tungsten lens-end lamps with a double filament, shapphire window and collecting optics. A dual filament provides enough illumination for the distant sample while reducing the number of lamps needed for module downsizing. A front-end lens guides more light from the filament to the sample target area. Sapphire windows are commonly employed as an optical windows in a variety of optical products due to its excellent optical characteristics from UV to IR, high strength, chemical inertness, and scratch resistance. Sapphire windows with anti-reflection coating in the specified operating range are recommended for incidence angles of less than 40 degrees to improve optical throughput, but the product’s cost will be increased slightly. In non-imaging optical systems, the interference fringes created by this optical window had little impact. Hence for non-imaging applications, optical window

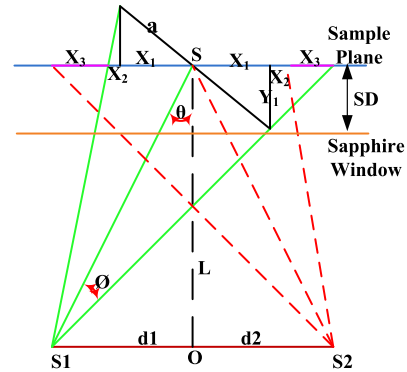


FIGURE 2. Illumination module geometry.

specifications such as 3.5 arc minutes parallelism and 2 arc minutes surface flatness are sufficient. Appropriate optics was used to capture more diffused light from the sample’s targeted active area and direct it to the polychromator. The SD of the sample, SAIA, and DOIR is determined mainly by the lamp emission angle, the angle between the lamp axis and sample plane, and the distance between two lamps in the geometry.

Multiple configurations were developed for the targeted standoff distance by using a set of equations referred to “1-to- 5”. By comparing numerous designs, an optimum illumination module geometry was determined using a lamp emission angle( $\phi$ ) of about  $17.3^\circ$ , an angle between the lamp axis and perpendicular to the sample plane( $\theta$ ) of about  $41^\circ$ , and a distance between two lamps ( $d1+d2$ ) of about 11.4mm, as shown in Fig.2. In Fig. 2, S1 and S2 - are lamp emission points, ‘ $\phi$ ’ - is lamp emission angle,  $d1+d2$  - is distance between emission points of two lamps, ‘L’ - is distance between Lamps plane to sample plane, ‘SD’ - is standoff distance between sapphire window to sample plane, ‘ $\theta$ ’ - is angle between lamp axis and perpendicular to the sample plane, ‘a’ - is lamp half illumination area at  $0^\circ$  angle, and  $x1,x2,x3$  - overlap and non-overlap areas created by two lamps, s1 and s2. The proposed modules and the NIRscan Nano EVM were simulated in Zemax using non-sequential ray-tracing method. In order to determine the DOIR and sample location for attaining maximum power, the illumination power at various standoff distances from the sapphire window was examined. Finally, the functional parameters of the proposed prototype using indigenized application software were evaluated.

Where  $X_1, X_2, X_3,$  and  $Y_1$  are:

$$X_1 = a \cos(\theta) \tag{1}$$

$$Y_1 = X_1 \tan(\theta) \tag{2}$$

$$X_2 = Y_1 / \tan((90-\theta) + (\phi)) \tag{3}$$

$$X_3 = Y_1 / \tan((90-\theta) - (\phi)) \tag{4}$$

$$\text{Overlap area at targeted sample plane} = 2(X_1 + X_2) \tag{5}$$

A larger standoff distance model requires a larger sample window, larger module size, and high-powered lamps. High-powered lamps consume a lot of power, making the

development of battery-powered devices a challenge. Increasing the sample window and device size allows for more stray light and increases the price. Factoring all these challenges in this analysis, we propose an optimized geometry to meet current needs without sacrificing efficiency.

## B. INSTRUMENT PERFORMANCE VALIDATION

Before allowing the instrument to establish a prediction model for sample analysis, it must first go through a series of tests to determine its functional parameters such as throughput (detectivity), SNR, baseline, repeatability, linearity, and accuracy. To compare and examine the impact of different geometrical illumination models on the results, throughput, SNR, and baseline measurements were done for both ELICO NIRS prototype and the NIRscan Nano EVM. The scan data in 'CSV' format allows the user to upload and download the spectra. Reference data was captured with a known diffuse reflectance standard (ref no. SRS-99, Labsphere) close to 99% reflection in the entire desired wavelength region.

### 1) THROUGHPUT (INTENSITY)

The throughput of both the ELICO prototype and the NIRscan Nano EVM was measured by capturing the NIR spectrum from a known standard diffuse reflectance standard.

### 2) SNR

Signal-to-noise ratio (SNR or S/N) is a measure that compares the level of the desired signal to the level of background noise. NIR spectrometer requires large SNR and is achieved by the collection of maximum light intensity. Large SNR allows detecting small changes on a large signal and provides more precise measurements. On both ELICO NIRS prototype and NIRscan Nano EVM, SNR is measured by recording 100 scans at 15 ms, 30 ms, and 60 ms integration times.

### 3) BASELINE

The initial baseline of the instrument is established by considering the effects of the environment and background noise. To get an accurate absorption profile, subtract the resultant baseline from the sample raw data. Next, a baseline test scan is performed at various gain settings across the entire wavelength range and compared for both instruments. Finally, the corrected signal for the peak-to-peak fluctuations is determined.

### 4) REPEATABILITY

The ELICO NIRS prototype's repeatability is studied using inter-day and intra-day variations. First, repeatability is measured by analyzing two different particle sizes of pure powder samples, such as chalk and red chili, and two different grain samples, such as wheat and groundnut. Then, all samples are analysed at different timing during one day for intra-day variations and the same procedure is followed for two different days to study the inter-day variations.

Data pre-processing is essential in analyzing the samples with different particle sizes and building a calibration

model in NIR spectroscopy analysis. With well-designed pre-processing techniques [26]–[28] such as scatter corrections and derivative techniques, the instrument's performance is greatly improved. To analyze the sample data for repeatability and linearity tests, we need to apply scatter correction techniques such as multiplicative scatter correction (MSC) and Standard Normal Variate (SNV) technique to minimise the scatter effects originating from path length differences and particle size.

For measuring repeatability with and without data pre-processing techniques, the percentage relative standard deviation (% RSD) of the concentration of 10 repeated scans of each sample has been taken in the multi-point scan method.

## 5) LINEARITY & ACCURACY

For studying the linearity and prediction accuracy of ELICO NIRS prototype, poultry feed samples were taken to analyze moisture content in feed formulation and the experiment collected around 100 samples from a feed manufacturing plant. On one set of the samples, we performed wet chemical analysis. On the second set, spectral measurements were taken using ELICO NIRS spectrometer having a range of 900 to 1700 nm. After taking the initial raw spectral measurements, the sample was spiked by adding moisture (water), then another spectral measurement was taken to obtain and validate the variation in moisture. After collecting raw data, pre-processing techniques were applied, and Partial Least Square Regression (PLSR) model was developed using calibration and validation sets for the spectral range of 950-1650 nm and a separate set was used for obtaining prediction accuracy.

## IV. RESULTS AND DISCUSSION

### A. OPTICAL DESIGN AND SIMULATION ANALYSIS

Using the Zemax non-sequential mode, an ELICO NIRS prototype and an NIRscan Nano EVM simulation model was designed to illuminate the sample at a specified standoff distance. A one-watt per lamp source was chosen for a standard model of NIRscan Nano EVM and two-watt per lamp source for the prototype of ELICO NIRS model. Sources were positioned at an optimum location and angle to achieve the necessary overlap region to illuminate the target sample position. We match the overlap of the active region and the optics vision cone by selecting the appropriate optics with "f/number."

A detector was placed at the sample location to determine radiometric output. This metric calculates the amount of illuminating power that reaches the active region. The physical properties of the lamps and the optics of the illumination module were redesigned and optimized. The design must improve to obtain the desired level of illumination power. The design was deemed satisfactory when the preferred metric reached maximum power at the target sample location. In Zemax non-sequential mode, accurate design analysis requires selecting the correct source, power distribution, and detector type. The source model determines the cone angle

and energy distribution of the light. Since the “detector rectangle” version is helpful for our analysis, there are several options for the detector type. This method allows the user to determine the number of pixels and sizes on the sensor. For an accurate study, the NIRscan Nano EVM’s detector size is 2.5 mm, and the ELICO NIRS prototype model’s detector size is 4 mm. The system design was set up in Zemax for analysis and run ray-trace simulation. After completing the ray trace, the irradiance at the detector plane was measured. The ray trace uses the detector viewer, allowing for different irradiance views. The resultant illumination module ray geometry of both models is shown in Fig. 3. The results from the Zemax simulation of various standoff distances against the sapphire window and the corresponding overlap area and illumination power are shown in Fig. 4.

As shown in Fig. 4, NIRscan Nano EVM provided a 2.5 mm SAIA and 66 percent light power to illuminate the sample at ‘0 mm’ position, allowing for accurate analysis. Because of the shallow depth of illumination, only 45 percent of the light energy was detected at a distance of 1 mm from the sapphire window, which was insufficient for precise measurements. Because of this geometry, the sample can be used for measurements up to 0.75 mm. The ELICO NIRS Prototype model increased SAIA by 4 mm and DOIR by 2 mm. Illumination power was 72 percent at ‘2.5 mm’ and 62 percent at ‘4.5 mm,’ and this range was used to keep the sample for reliable analysis.

### B. IMPROVED GEOMETRICAL PARAMETERS

Table-1 shows the improved geometrical parameters of ELICO NIRS prototype compared to NIRscan Nano EVM model. The ELICO NIRS prototype model modified the angle and orientation of the two lens-end double filament lamps to achieve the desired 3.5 mm standoff distance against the sapphire window for accurate scanning of the sample. Both lamps formed an SAIA of 4.0 mm at the sample position, coinciding with the collection optics’ vision angle. To maximize optical throughput, the field angle from SAIA on the object side and the spectrometer’s “f/number” (NIRnano Scan EVM) and slit size on the image side are used to determine appropriate and effective focal length as well as clear aperture for designing collection optics. This configuration prevents stray light from entering the spectrometer and reduces its effect on accurate measurements. As the angle between the lamp axis and the vertical axis of the sample plane decreases, the DOIR increases. ELICO NIRS prototype geometry achieved a maximum DOIR of 2 mm to access the sample position without significantly affecting measurement accuracy. Fig. 3 shows the ray geometry of an illumination module, illustrating the geometric variations of the proposed model and the NIRscan Nano EVM.

### C. MULTI-POINT SCAN WITH ELICO NIRS PROTOTYPE

The ELICO NIRS prototype consists primarily of a newly developed illumination module, the NIRscan Nano EVM’s polychromator, and a microcontroller that allows for

**TABLE 1. Improved optical geometry parameters of illumination module: NIRnano scan EVM vs. ELICO NIRS prototype.**

Parameter	NIRscan Nano EVM	Prototype
<b>SD:</b> Standoff Distance	0.0 mm	3.5 mm
<b>SAIA:</b> Sample Active Illumination Area	2.5 mm	4.0 mm
<b>DOIR:</b> Depth of Overlap Illumination Region	0.75 mm	2.0 mm

multi-point scanning of the bulk sample at various points while rotating the sample holder. The proposed geometry of the illumination module allows for 3.5 mm of space for the rotation mechanism, sample holder, and sample. As a result, the measuring device illuminates the sample sufficiently and takes several measurements as the sample holder rotates, ensuring that the measurement is as homogeneous as possible.

### D. PERFORMANCE OF ELICO NIRS PROTOTYPE

The prototype’s performance is validated in terms of throughput, baseline, SNR, repeatability, linearity, and accuracy.

#### 1) THROUGHPUT (INTENSITY)

Throughput was measured by using a standard diffuse reflectance. The scan was performed to obtain NIR spectrum scan of a known diffuse reflectance standard on NIRscan Nano EVM and ELICO NIRS Prototype. Fig. 5(a) shows the output intensity curves for both models. The abscissa is the wavelength, and the ordinate is the relative power strength in analog units. The output intensity of NIRscan Nano EVM is red, while the output intensity of ELICO NIRS prototype model is blue. In comparison to the output intensities of both models, the resulting intensity, as illustrated in Fig. 5(b), is calculated as the ratio of differences in output intensities of both models to output intensity of one model, then multiplied by 100. The proposed ELICO NIRS prototype geometry increases the intensity of the output by a factor of 2-3.

#### 2) BASELINE

A baseline test scan is performed at various gains across the entire wavelength spectrum and compared for both instruments. Finally, the corrected signal is evaluated for peak-to-peak fluctuations. The NIRscan Nano EVM achieved  $< \pm 0.005\text{Abs}$  in all gain settings, whereas ELICO NIRS prototype achieved  $< \pm 0.003\text{Abs}$  at gain-1 and  $< \pm 0.001\text{Abs}$  at gain-16 & 64, and the results are shown in Fig. 6 (a, b, & c). Finally, ten consecutive baseline scans were performed, and the data was captured using ELICO NIRS prototype model. All the baseline scans within  $< \pm 0.003\text{Abs}$  as shown in Fig. 6(d).

#### 3) SNR

SNR calculations were performed on ELICO prototype and NIRscan Nano EVM, with 100 scans captured on both models

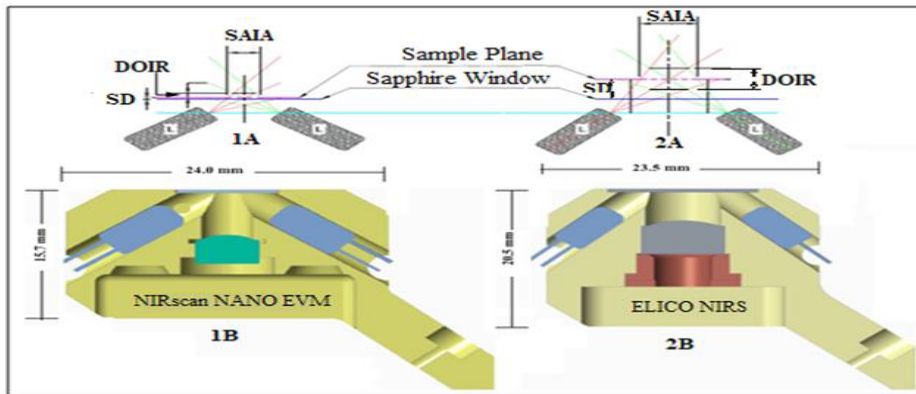


FIGURE 3. Illumination module - Ray geometry: (1A). NIRscan nano EVM; (2A). ELICO NIRS prototype outer dimensional layout: (1B). NIRscan nano EVM; (2B). ELICO NIRS prototype.

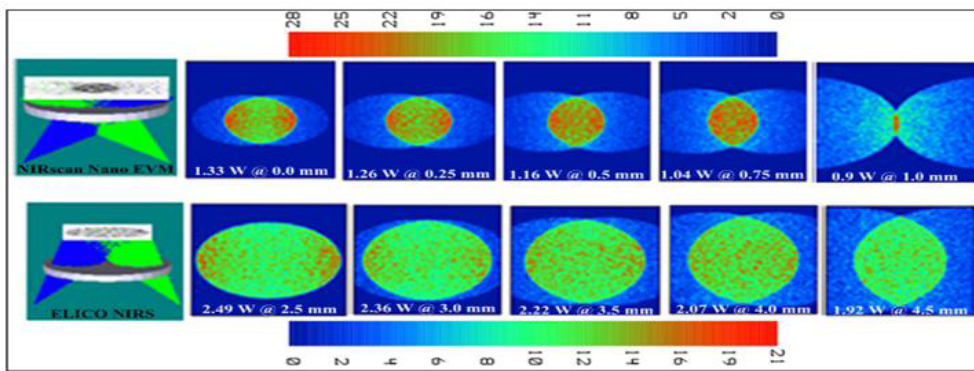


FIGURE 4. Zemax simulation: Resultant power @ various standoff distances using NIRscan nano EVM and ELICO NIRS prototype.

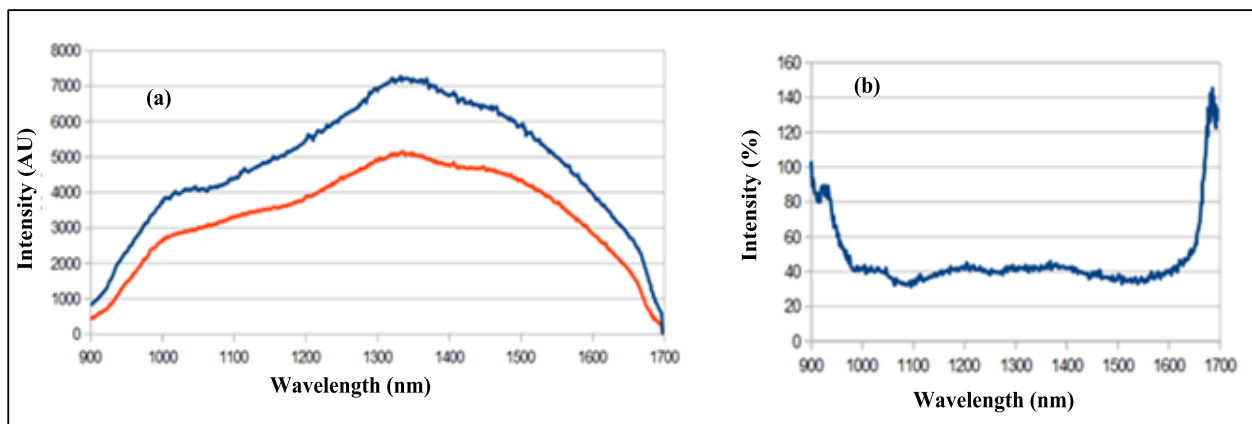


FIGURE 5. Optical throughput graph: (a) comparative intensity study profiles of NIRscan nano EVM and ELICO NIRS prototype and (b) intensity enhanced difference profile.

at 15 ms, 30 ms, and 60 ms integration times, and SNR was determined using the formula below,

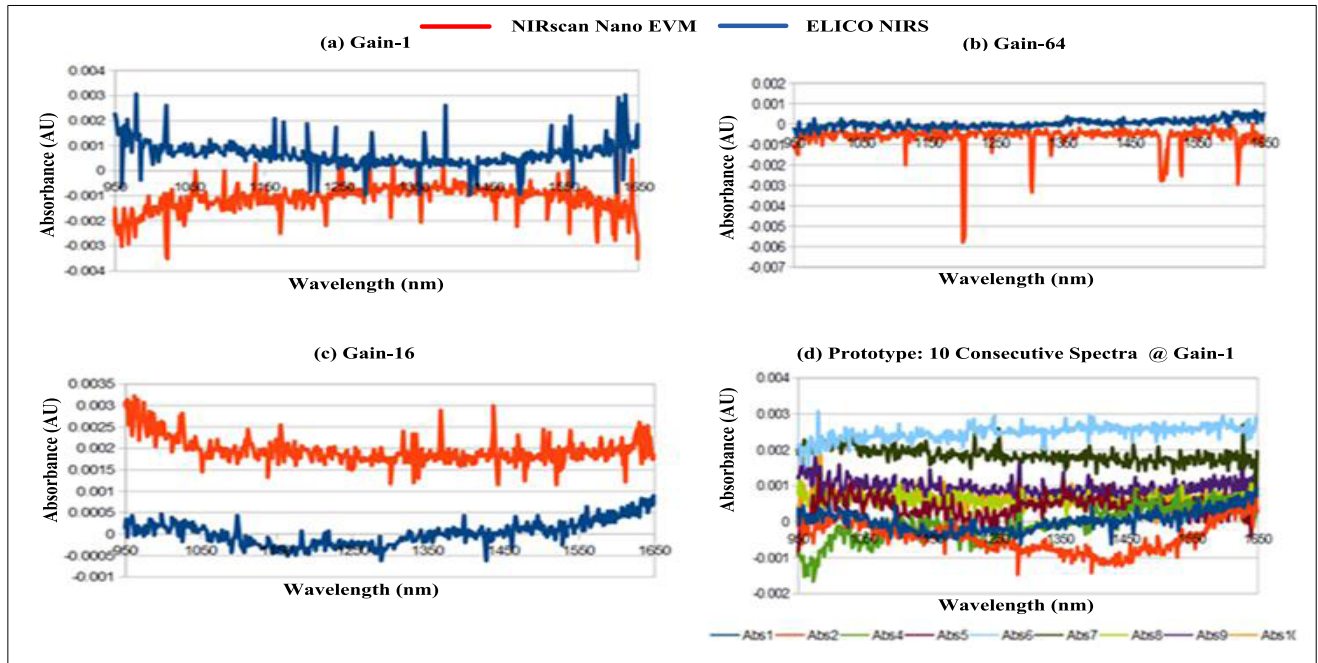
$$SNR = \frac{\sum_{m=1}^k (Int[\lambda_n, s_m]) / k}{\sqrt{\sum_{m=2}^k (Int[\lambda_n, s_{m-1}]) / k - 1}} \quad (6)$$

Table 2 shows that the proposed ELICO NIRS prototype geometry increased throughput, baseline, and SNR compared to NIRscan Nano EVM. In addition, further study showed that

the Limit-of-Detection (LOD) and instrument sensitivity had greatly improved.

#### 4) REPEATABILITY

Repeatability experiment was performed for inter-day and intra-day and this was evaluated to determine how repeatable instrument results are under a set of similar conditions. Repeatability was determined by analyzing pure powder and grain samples' spectral data using the multi-point scan method. The result % amount found was between 99% and



**FIGURE 6.** Baseline spectra of NIRscan nano EVM (Red) and ELICO NIRS (blue) @ various gains: (a) Gain-1, (b) Gain-16, (c) Gain-64, and (d) 10 consecutive spectra captured from ELICO NIRS prototype at Gain-1.

**TABLE 2.** Improved instrument performance parameters: NIRscan nano EVM vs. ELICO NIRS prototype.

Parameter		TI NIRscan Nano EVM	ELICO NIRS Prototype
Throughput (Intensity) @ 1350nm		5000 AU	7000 AU
Baseline		$<\pm 0.005$	$<\pm 0.003$
SNR @ Peak Wavelength	15ms	60 <sup>1</sup>	1900 <sup>1</sup>
	30ms	250 <sup>1</sup>	2500 <sup>1</sup>
	60ms	7000 <sup>2</sup>	10000 <sup>2</sup>

Note 1- DMD Pattern width considered as 2.34nm

Note 2- DMD Pattern width considered as 23.4nm

101% with %RSD <1% by applying MSC. As shown in Table-3, results indicate that this prototype is precise for the determination of the quality of the food samples using multi-point scan method.

5) LINEARITY & ACCURACY

Poultry feed samples with moisture in the range of 10 to 20% were scanned on an ELICO NIRS prototype using a multi-point scan technique. As shown from the original raw spectrum in Fig. 7, there is a significant drift; although the spectra are similar overall. Significant drift in NIR raw spectral data is caused by incremental moisture level, instrumentation base noise, sample particle size and orientation, and sample particle spacing. Therefore, to extract better moisture content results, the raw spectra were subjected to

**TABLE 3.** Repeatability studies of ELICO NIRS prototype on 100% pure samples.

Sample	Pre-Process Techniques	Intra-Day		Inter-Day	
		STDE V	% RSD	STDE V	% RSD
Chalk	No treatment	0.0011	0.82	0.002	1.03
	MSC	0.00073	0.15	0.0011	0.185
Red Chili	No treatment	0.0031	0.44	0.0023	0.42
	MSC	0.0016	0.36	0.0018	0.28
Wheat	No treatment	0.0041	1.13	0.0052	1.29
	MSC	0.0025	0.62	0.0013	0.6
Groundnut	No treatment	0.056	10.67	0.081	18.53
	MSC	0.0012	0.71	0.0016	0.95

Note: Average of 10 Estimates

Savitzkey-Golay smoothing, SNV or MSC, and first derivative to establish a robust quantitative model. These techniques increase contrast and aid in the resolution of overlapping moisture content peaks. After applying the pre-processing techniques discussed above to the raw spectral data shown in Fig. 7, Fig. 8 depicts the resulting linear variation at 1450nm for each moisture level.

To compute the moisture content of the feed sample, we applied raw spectral data, well-pre-processing techniques, and partial least square regression (PLSR) to develop better calibration and validation statistical prediction equations. Correlation coefficient ( $R^2$ ), cross-validation root

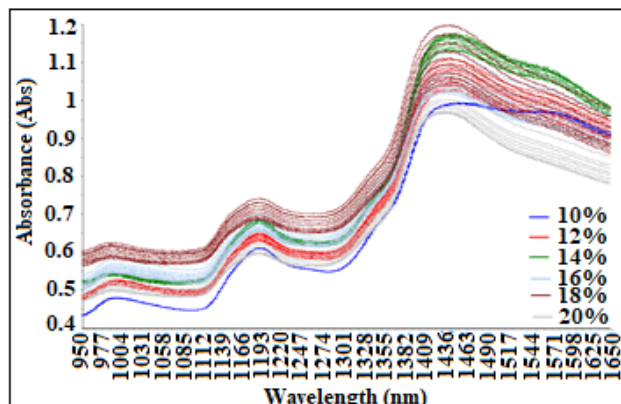


FIGURE 7. Raw NIR spectra of poultry feed samples for the moisture range of 10–20%.

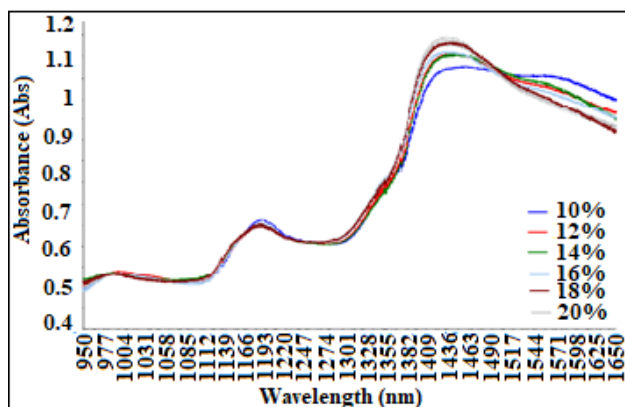


FIGURE 8. MSC applied NIR spectra of poultry feed samples for the moisture range of 10–20%.

TABLE 4. The PLSR modeling results after applying various pre-processing techniques.

Pre-Process Techniques	R <sup>2</sup>	RMSECV	RMSEP
Raw Data -No Treatment	0.927	0.92	1.11
MSC	0.986	0.27	0.42
SNV	0.947	0.64	0.86
MSC- 1st Derivative	0.991	0.25	0.32

mean square error (RMSECV), prediction root mean square error (RMSEP) were used as evaluation criteria. The smaller the RMSE value and the closer R<sup>2</sup> value to 1, the greater the correlation between the real and predicted values. Table 4 shows the results of different pre-process techniques after PLSR modeling. The results show that the model that uses the first derivative is better than other pre-process techniques. Fig. 9 shows the resulting moisture content of each sample in the calibration set plotted against the wet chemistry values. The moisture content prediction model produced had an excellent R<sup>2</sup> of 0.9915, RMSECV of 0.247, and RMSEP of 0.324 percent.

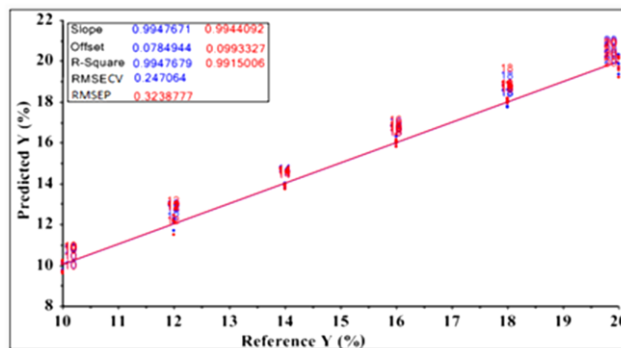


FIGURE 9. Prediction model was developed using PLSR for calibration set of poultry feed samples for the moisture range of 10–20%.

TABLE 5. Prediction accuracy results of the ELICO NIRS prototype.

Sample	Reference Value (%)	Predicted Value (%)	%-Deviation
1	10	10.61	0.30
2	10	10.75	0.32
3	12	12.24	0.33
4	12	12.46	0.37
5	14	14.49	0.31
6	14	14.38	0.40
7	16	15.15	0.38
8	16	15.23	0.33
9	18	17.08	0.64
10	18	16.96	0.67
11	20	18.68	0.76
12	20	18.22	0.87

The evaluation parameters are reasonable, so this study used modeling result as the final result. The prediction set samples were predicted using the above model, and the predicted results were compared with the standard wet chemical values, as shown in Table-5. It can be seen from the results that the maximum percent of deviation of the system is less than 1%, and the minimum is 0.3%. Thus, in this study, ELICO NIRS prototype shows that it has high prediction ability for multi-point scan analysis and can be applied for rapid detection of standoff distant heterogeneous samples and is suitable for use in labs of food industries where users can obtain results quickly and accurately.

### V. CONCLUSION

This paper presents ELICO NIRS prototype illumination module using the NIRscan Nano EVM to perform multi-point scan analysis of standoff distant samples. The proposed module’s geometry improved optical characteristics in terms of SD, SAIA, and DOIR. The standoff distance (SD) achieved is about 3.5 mm, allowing standard sample holders to retain the sample for a single-point scan and a sample rotation mechanism for multi-point scan analysis. The prototype model achieves an SAIA with a maximum intensity of 4.0 mm at a standoff distance of 3.5 mm from the sapphire window by improving optical geometry. It improves detectivity by a factor of 2 - 3 by collecting maximum diffused reflection



light from the sample by proper collection optics. The DOIR increased to 2 mm, allowing the sample's position without compromising the accuracy of the analysis. The evaluation results show a noticeable improvement in instrument baseline of around  $< \pm 0.003$  Abs at gain 1 and  $< \pm 0.001$  Abs at gain 16. The study's findings revealed a low-cost portable instrument with improved signal to noise ratio (SNR) and limit of detection (LOD), as well as the ability to conduct multi-point analysis on bulk, inhomogeneous, and heterogeneous samples. PLSR analysis on a data set of feed samples with moisture ranges of 10–20% percent yielded a prediction model with acceptable precision, with an  $R^2$  of 0.991 and a prediction error of 0.32 percent. ELICO NIRS prototype prediction values of a feed sample highly correlated with wet chemistry method's values, with a maximum deviation of  $< 1\%$ . Therefore, it can be concluded that the ELICO NIRS is sensitive and is ready to read distinctive variations levels in the feed samples in our lab setup. Since the ELICO prototype is cost-effective and generates results rapidly, feed manufacturers can maintain tight control and monitor what is going into the finished feed, thereby reducing production losses during the manufacturing process. According to this section of the fundamental study, the ELICO NIRS prototype combined with chemometrics has vast potential as a stand-alone or in-line monitoring tool for food applications.

## ACKNOWLEDGMENT

The authors would like to thank Prof. D. Dinakar, Head, Department of Physics, National Institute of Technology (NIT), Warangal, Telangana, and the researchers of the Research and Development Division, ELICO Ltd., Hyderabad, Telangana, for their valuable support during this research.

## REFERENCES

- [1] G. Downey, "Authentication of food and food ingredients by near infrared spectroscopy," *J. Near Infr. Spectrosc.*, vol. 4, no. 1, pp. 47–61, Jan. 1996, doi: [10.1255/jnirs.75](https://doi.org/10.1255/jnirs.75).
- [2] L. Chen, Z. Yang, and L. Han, "A review on the use of near-infrared spectroscopy for analyzing feed protein materials," *Appl. Spectrosc. Rev.*, vol. 48, no. 7, pp. 509–522, 2013, doi: [10.1080/05704928.2012.756403](https://doi.org/10.1080/05704928.2012.756403).
- [3] C. Kumaravelu and A. Gopal, "A review on the applications of near-infrared spectrometer and chemometrics for the agro-food processing industries," in *Proc. IEEE Technol. Innov. ICT Agricult. Rural Develop. (TIAR)*, Jul. 2015, pp. 8–12, doi: [10.1109/TIAR.2015.7358523](https://doi.org/10.1109/TIAR.2015.7358523).
- [4] M. Mohamad, A. R. Msabbri, and M. Z. MatJafri, "Conceptual design of near infrared spectroscopy instrumentation for skin moisture measurement," in *Proc. IEEE Colloq. Humanities, Sci. Eng.*, Dec. 2011, pp. 801–804, doi: [10.1109/CHUSER.2011.6163846](https://doi.org/10.1109/CHUSER.2011.6163846).
- [5] W. Tao and W. Xiaofei, "Study on germination of tomato seed based on near-infrared spectroscopy," in *Proc. IEEE 11st Int. Conf. Electron. Meas. Instrum.*, Aug. 2013, pp. 291–293, doi: [10.1109/ICEMI.2013.6743025](https://doi.org/10.1109/ICEMI.2013.6743025).
- [6] O. Abbas, A. Pissard, and V. Baeten, "Near-infrared, mid-infrared, and Raman spectroscopy," in *Chemical Analysis of Food*. New York, NY, USA: Academic, 2020, pp. 77–134, doi: [10.1016/B978-0-12-813266-1.00003-6](https://doi.org/10.1016/B978-0-12-813266-1.00003-6).
- [7] Y. Ozaki, A. Ikehata, and H. Shinzawa, "Near-infrared spectroscopy in biological molecules and tissues. European biophysical societies," in *Encyclopedia of Biophysics*. Berlin, Germany: Springer, 2018, doi: [10.1007/978-3-642-16712-6\\_138](https://doi.org/10.1007/978-3-642-16712-6_138).
- [8] J. B. Johnson, "An overview of near-infrared spectroscopy (NIRS) for the detection of insect pests in stored grains," *J. Stored Products Res.*, vol. 86, Mar. 2020, Art. no. 101558, doi: [10.1016/j.jspr.2019.101558](https://doi.org/10.1016/j.jspr.2019.101558).
- [9] X. Du, J. Wang, D. Dong, and X. Zhao, "Development and testing of a portable soil nitrogen detector based on near-infrared spectroscopy," in *Proc. IEEE 8th Joint Int. Inf. Technol. Artif. Intell. Conf. (ITAIC)*, May 2019, pp. 822–826, doi: [10.1109/ITAIC.2019.8785499](https://doi.org/10.1109/ITAIC.2019.8785499).
- [10] H. Yan and H. W. Siesler, "Hand-held near-infrared spectrometers: State-of-the-art instrumentation and practical applications," *NIR News*, vol. 29, no. 7, pp. 8–12, Nov. 2018, doi: [10.1177/0960336018796391](https://doi.org/10.1177/0960336018796391).
- [11] C.-H. Chen, C.-W. Chen, T.-S. Liao, and C.-H. Hwang, "A design of near infrared spectrometer for pears sugar concentration analysis," in *Proc. IEEE Instrum. Meas. Technol. Conf.*, May 2010, pp. 1377–1381, doi: [10.1109/IMTC.2010.5488265](https://doi.org/10.1109/IMTC.2010.5488265).
- [12] G. R. Fernandez, J. L. Matias, F. Ferrero, M. Villedor, J. C. Campo, L. Royo, A. Soldado, and S. Forcada, "Portable IoT NIR spectrometer for detecting undesirable substances in forages of dairy farms," in *Proc. Int. Conf. Sens. Instrum. IoT Era (ISSI)*, Aug. 2019, pp. 1–6, doi: [10.1109/ISSI47111.2019.9043656](https://doi.org/10.1109/ISSI47111.2019.9043656).
- [13] R. Cama-Moncuñill, M. Markiewicz-Keszycka, Y. Dixit, X. Cama-Moncuñill, M. P. Casado-Gavalda, P. J. Cullen, and C. Sullivan, "Multipoint NIR spectroscopy for gross composition analysis of powdered infant formula under various motion conditions," *Talanta*, vol. 154, pp. 423–430, Jul. 2016, doi: [10.1016/j.talanta.2016.03.084](https://doi.org/10.1016/j.talanta.2016.03.084).
- [14] E. J. Wolfrum, C. Payne, A. Schwartz, J. Jacobs, and R. W. Kressin, "A performance comparison of low-cost near-infrared (NIR) spectrometers to a conventional laboratory spectrometer for rapid biomass compositional analysis," *BioEnergy Res.*, vol. 13, pp. 1–9, May 2020, doi: [10.1007/s12155-020-10135-6](https://doi.org/10.1007/s12155-020-10135-6).
- [15] A. Kauppinen, M. Toivaiainen, M. Lehtonen, K. Järvinen, J. Paaso, M. Juuti, and J. Ketolainen, "Validation of a multipoint near-infrared spectroscopy method for in-line moisture content analysis during freeze-drying," *J. Pharmaceutical Biomed. Anal.*, vol. 95, pp. 229–237, Jul. 2014, doi: [10.1016/j.jpba.2014.03.008](https://doi.org/10.1016/j.jpba.2014.03.008).
- [16] Y. Dixit, M. P. Casado-Gavalda, R. Cama-Moncuñill, P. J. Cullen, and C. Sullivan, "Challenges in model development for meat composition using multipoint NIR spectroscopy from at-line to in-line monitoring," *J. Food Sci.*, vol. 82, no. 7, pp. 1557–1562, Jul. 2017, doi: [10.1111/1750-3841.13770](https://doi.org/10.1111/1750-3841.13770).
- [17] Y. Dixit, M. P. Casado-Gavalda, R. Cama-Moncuñill, X. Cama-Moncuñill, F. Jacoby, P. J. Cullen, and C. Sullivan, "Multipoint NIR spectrometry and collimated light for predicting the composition of meat samples with high standoff distances," *J. Food Eng.*, vol. 175, pp. 58–64, Apr. 2016, doi: [10.1016/j.jfoodeng.2015.12.004](https://doi.org/10.1016/j.jfoodeng.2015.12.004).
- [18] R. Cama-Moncuñill, Y. Dixit, X. Cama-Moncuñill, M. P. Casado-Gavalda, M. Markiewicz-Keszycka, P. J. Cullen, and C. Sullivan, "Multipoint NIR spectroscopy for simultaneous analyses of dairy products—Part B: Quantification," *NIR news*, vol. 28, no. 5, pp. 13–16, Aug. 2017, doi: [10.1177/0960336017715863](https://doi.org/10.1177/0960336017715863).
- [19] M. Boiret and F. Chauchard, "Use of near-infrared spectroscopy and multipoint measurements for quality control of pharmaceutical drug products," *Anal. Bioanal. Chem.*, vol. 409, no. 3, pp. 683–691, Jan. 2017, doi: [10.1007/s00216-016-9756-9](https://doi.org/10.1007/s00216-016-9756-9).
- [20] R. Hohl, O. Scheibelhofer, E. Stocker, S. S. Behzadi, D. Haack, K. Koch, P. Kerschhaggl, D. Lochmann, S. Sacher, and A. Zimmer, "Monitoring of a hot melt coating process via a novel multipoint near-infrared spectrometer," *AAPS PharmSciTech*, vol. 18, no. 1, pp. 182–193, Jan. 2017, doi: [10.1208/s12249-016-0504-4](https://doi.org/10.1208/s12249-016-0504-4).
- [21] P. Nelson, "DLP technology for spectroscopy," Texas Instrum., Dallas, TX, USA, Tech. Rep., 2014. [Online]. Available: <https://www.ti.com/lit/pdf/dlpa048>
- [22] *DLP NIRscan Nano EVM User's Guide*. Texas Instrum., Dallas, TX, USA, Aug. 2017.
- [23] U. Mantena, "Apparatus and method for multipoint analysis of standoff distant analyte using near infrared spectrometer," Indian Patent Appl. 2021 41 008 449, Mar. 1, 2021.
- [24] C. Pasquini, "Near infrared spectroscopy: Fundamentals, practical aspects and analytical applications," *J. Brazilian Chem. Soc.*, vol. 14, no. 2, pp. 198–219, Apr. 2003, doi: [10.1590/S0103-50532003000200006](https://doi.org/10.1590/S0103-50532003000200006).
- [25] G. Perrella, "Texas instruments DLP NIRscan nano evaluation module (EVM) optical design considerations," Texas Instrum., Dallas, TX, USA, Appl. Rep. DLPA062, Jan. 2016.
- [26] H. Mark, "Chemometrics in near-infrared spectroscopy," *Analytica Chimica Acta*, vol. 223, pp. 75–93, Jan. 1989, doi: [10.1016/S0003-2670\(00\)84075-1](https://doi.org/10.1016/S0003-2670(00)84075-1).

- [27] Y. A. Purwanto, H. P. Sari, and I. W. Budiastira, "Effects of preprocessing techniques in developing a calibration model for soluble solid and acidity in 'Gedong Gincu' mango using NIR spectroscopy," *Int. J. Eng. Technol.*, vol. 7, no. 5, pp. 1921–1927, 2015.
- [28] H. Martens and E. Stark, "Extended multiplicative signal correction and spectral interference subtraction: New preprocessing methods for near infrared spectroscopy," *J. Pharmaceutical Biomed. Anal.*, vol. 9, no. 8, pp. 625–635, 1991, doi: 10.1016/0731-7085(91)80188-f.



**SOURABH ROY** was born in Dakshin Dinajpur, West Bengal, India, in February 1982. He received the B.Sc. and M.Sc. degrees in physics from the University of North Bengal, West Bengal, in 2002 and 2004, respectively, and the Ph.D. degree in physics from the Indian Institute of Technology Kharagpur, India, in 2010. He then pursued his postdoctoral research with the CNIT–University of Padova, Italy, as a Postdoctoral Researcher under the project EU-FP7 Governing the Speed of Light (GOSPEL). In 2012, he joined as a Faculty Member of physics at the NIT, Warangal, where he is currently working as an Associate Professor. He is the author/coauthor of over 25 research papers. His research interests include photonic crystals, nonlinear optics, fiber Bragg grating sensors, photonic devices, and sensors. He is also an active member and a Faculty Advisor of the SPIE Student Chapter at NIT, Warangal.



**UMACHANDI MANTENA** was born in Vijayawada, Andhra Pradesh (AP), India, in August 1980. She received the B.Sc. degree from Acharya Nagarjuna University, Guntur, AP, in 2000, and the M.Sc. (Tech.) degree in engineering physics (photonics) from the National Institute of Technology (NIT)-Warangal, Kakatiya University, Telangana, India, in 2004, where she is currently pursuing the Ph.D. degree. She is currently a Sr. Optics Design Engineer with the Department of Research and Development, ELICO Ltd., Hyderabad, Telangana. Her research interests include fundamental investigation and application of spectrometers, especially in the optical design of imaging and non-imaging optical systems.



**RAMESH DATLA** received the Bachelor's Degree in Electronics and Communication Engineering from Osmania University, India, a Postgraduate Degree in Electronic Design Technology from Indian Institute of Science, Master's Degree in Electrical Engineering from Wichita State University, USA, Graduate in Executive Management from the MIT Sloan School of Business, USA, and a Ph.D. degree in Spectroscopy Instrumentation from Sri Krishnadevaraya University, India. He is currently the Chairperson of ELICO Ltd., an Analytical Instrumentation Design and Manufacturing Company, and also the Chairperson of the Confederation of Indian Industry National Committee on Intellectual Property Rights. He specializes in Applied Research in the area of Spectroscopy Instrumentation and Advocacy in Intellectual Property Rights.

• • •